Int. J. Appl. Math. Comput. Sci., 2025, Vol. 35, No. 3, 467–477
DOI: 10.61822/amcs-2025-0033

DOPPLER SHIFT DETERMINATION METHODS DEDICATED TO MBFSK MODULATION

AGNIESZKA CZAPIEWSKA [a], ANDRZEJ ŁUKSZA [b], JAN H. SCHMIDT [a], RYSZARD STUDAŃSKI [b], ŁUKASZ WOJEWÓDKA [b,*], ANDRZEJ ŻAK [c]

[a]Faculty of Electronics, Telecommunications and Informatics
Gdańsk University of Technology
ul. G. Narutowicza 11/12, 80-233 Gdańsk, Poland
e-mail: {agnieszka.czapiewska, jan.schmidt}@pg.edu.pl

[b]Faculty of Electrical Engineering
Gdynia Maritime University
ul. Morska 81-87, 81-255 Gdynia, Poland
e-mail: {a.luksza, r.studanski, l.wojewodka}@we.umg.edu.pl

[c]Faculty of Mechanical and Electrical Engineering
Polish Naval Academy
ul. Śmidowicza 69, 81-127 Gdynia, Poland
e-mail: a.zak@amw.gdynia.pl

The progressive development of AUVs (Autonomous Underwater Vehicles) is creating demand for wireless underwater communications. The most commonly used transmission medium in water is acoustic wave. Unfortunately, the underwater hydroacoustic channel is characterized by strong multipath, especially in shallow reservoirs and in combination with hydrotechnical infrastructure. In addition, there is a Doppler effect in the case of reciprocal movement of the transmitting and receiving parts. This effect in a hydroacoustic channel causes a significant frequency shift due to the relatively low propagation speed of the acoustic wave. Knowledge of the frequency of the received signal is crucial in the reception process. The authors of the current publication have found through a number of studies that the MBFSK (Multiple Binary Frequency Shift Keying) modulation provides relatively high transmission bit rates in a multipath channel. In the current publication, two Doppler factor estimation methods dedicated to this modulation are presented: the double DFT and the correlation method. These methods were tested with utilization of signals recorded in real environment under conditions of strong multipath in motion. Research was conducted at the speeds of 0.5, 1 and 1.5 m/s between the transmitter and receiver. The results show that the proposed methods have comparable Doppler shift estimation quality to the well-known pilot method, without decreasing the bandwidth allocated for data transmission.

Keywords: underwater communication, multipath channels, Doppler shift, Doppler measurement, MBFSK.

1. Introduction

The underwater environment poses significant challenges to wireless communications due to the harsh propagation conditions resulting from the variability of the physical and chemical properties and the high signal attenuation. The primary medium used for underwater communications is elastic waves. Hydroacoustic signals are subject to many physical phenomena such as reflection, refraction and diffraction, which are the cause of multipath, the problem is widely described by Bjørnø and Buckingham (2017). The effectiveness of these waves varies depending on factors such as reservoir characteristics, presence of underwater obstacles, bottom type, water depth, weather conditions, water stratification and physicochemical properties. Two major problems to achieving high throughput and low error rate underwater communications are multipath propagation and the

*Corresponding author

Doppler effect.

Multipath interference is caused by multiple reflections of the acoustic wave from different underwater obstacles or structures. The Doppler effect occurs when there is relative motion between the transmitter and receiver, resulting in a frequency shift. Due to the low speed of wave propagation (1500 m/s), even relatively slow motion of the receiver and transmitter will cause a large frequency shift. This problem is more pronounced in broadband systems, where frequency shifts at the edges of the spectrum can vary significantly. The interaction of these phenomena causes that the reception point is reached by multiple different paths, each with a different Doppler frequency shift.

This results in frequency shifts and blurring of the signal in the frequency domain, making underwater communications significantly more difficult or even impossible. Specialized modulation techniques and additional processing are required to overcome these problems. One such modulation technique that is relatively resistant to multipath effects is MBFSK (Multiple Binary Frequency Shift Keying) (Mizeraczyk *et al*., 2021). This is because MBFSK relies on the amplitude spectrum of the signal for decision making, making it less sensitive to the paths the signal takes to reach the receiver. However, MBFSK is not immune to Doppler shifts, which affect the frequency domain of the carriers used for data transmission. In addition, multipath propagation can blur the spectrum of these carriers, making it difficult to identify them accurately. To ensure correct reception, additional processing is required, including the determination of the carrier frequency correction factor, which can be estimated using various methods. It would be good if these methods were relatively computationally simple, i.e., not demanding in terms of memory and computing power. In addition, and this seems crucial, it would be good if they did not take up the time and bandwidth available for data transmission.

In general, scientific literature frequently addresses subjects concerning the Doppler effect in acoustic wave-based wireless underwater communication. The knowledge of the Doppler is not only required during establishing link in communication systems (Talarczyk, 2023) but also is required in underwater navigation and localization systems (Ostrowski *et al*., 2020). In the vast majority of cases, chirp signals (Diamant *et al*., 2012), especially linear (Sharif *et al.*, 1999, 2000; Perrine *et al.*, 2010) or hyperbolic (Zhao *et al*., 2019; Wei *et al*., 2020), are used to determine the Doppler shift. In these scenarios, the time difference between two chirp signals sent with a specific interval is measured, and this difference is used to compute the Doppler shift, which then enables the correction of the received signal (Jin *et al*., 1995). The correction usually consists of resampling the received signal (Ma *et al*., 2020; Wada *et al*., 2016) although there are other approaches, such as that of Johnson *et al*. (1997), who proposes the use of RLS (Recursive Least Squares) filtering and PLLs (Phase-Locked Loops). Sun *et al*. (2022) use Kalman filtering for Doppler estimation and correction. On the other hand, in the paper by Jin *et al*. (1995), based on test data, a correction of the Doppler phenomenon is selected so that the minimum value of the bit error rate is obtained. Sun *et al.* (2023; 2020) and Baldone *et al*. (2020) suggest employing multi-channel correlation combined with various Doppler shifts to approximate Doppler shifts. In a similar vein, Mason *et al*. (2008) describe a method for estimating the Doppler effect by analyzing two identical OFDM (Orthogonal Frequency-Division Multiplexing) symbols with a cyclic prefix, using a receiver equipped with a bank of parallel autocorrelators tuned to different Doppler scaling factors. Another widely used approach involves utilizing pilot signals to estimate the Doppler effect, as discussed by Perrine *et al*. (2010), Nguyen *et al*. (2022) and Czapiewska *et al*. (2024b). However, it should be noted that most of the publications deal with hydroacoustic signal propagation in conditions where multipath effect does not occur or is negligible (Sharif *et al.*, 1999; Sun *et al.*, 2022; 2023; Baldone *et al.*, 2020; Nguyen *et al.*, 2022; Li *et al.*, 2019; 2008). Some research has been carried out under simulation conditions (Jin *et al*., 1995; Eynard and Laot, 2008; Liu *et al*., 2023; Deguchi *et al*., 2022) and some under real conditions (Sharif *et al*., 1999; Baldone *et al*., 2020; Nguyen *et al*., 2022; Li *et al*., 2008). The problem of multipath propagation in a small container such as a swimming pool is presented by Misiurewicz *et al*. (2021).

The aim of our work is to develop new Doppler shift determination methods for MBFSK modulation and to evaluate their suitability under strong multipath conditions. Therefore, in this paper we present two new methods, namely the double DFT and the correlation method, and we perform a series of experiments under real, very difficult propagation conditions, i.e., strong multipath with long channel memory time and reciprocal motion of transmitter and receiver.

The main contribution of this paper is the presentation of two new methods dedicated to MBFSK modulation that allow the determination of the Doppler factor. These two methods have some advantages, but the most important is that they use directly transmitted data in the MBFSK signal, without the necessity of additional signals that will reduce the throughput by consuming time or bandwidth. Another important contribution of the article is the evaluation of these methods in the real, multipath environment.

The paper has the following organization Section 2 describes in detail the modulation technique used in the research. In Section 3, the proposed Doppler estimation algorithms are presented. Section 4 describes

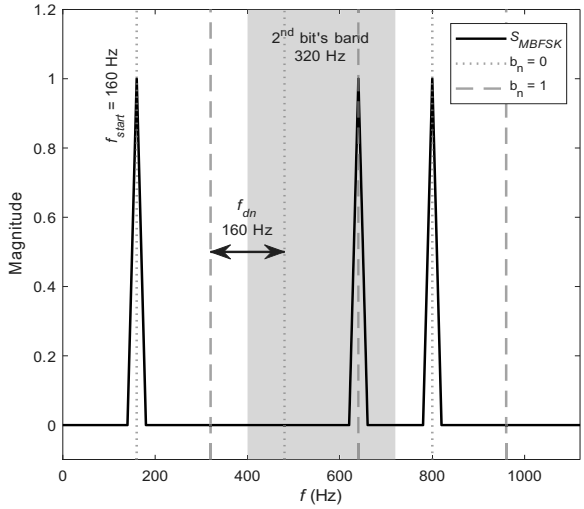

Fig. 1. Spectrum of an example MBFSK signal with $f_{start} = 160$ Hz, $f_{dn} = 160$ Hz, $N = 3$ in the case of transmitting [0, 1, 0] bits. Dotted vertical lines indicate the frequencies of the [0] bits and dashed lines indicate the frequencies of the [1] bits.

the measurement setup used during the laboratory runs, including the equipment and the transmission environment. Finally, Section 5 presents the results and a comparison of the methods.

2. Modulation technique

To create a wireless communication system that could operate in harsh multipath propagation conditions over short distances of up to 100 m while moving, the authors of this article selected MBFSK modulation. This modulation involves frequency multiplication of BFSK modulation. A $\boldsymbol{f_{mesh}}$ frequency grid is created in which there are N pairs of subcarriers corresponding to N transmitted bits (1).

$$\boldsymbol{f_{mesh}} = f_{start} + [0, f_{dn}, 2f_{dn}, \ldots, (2N-1)f_{dn}], \quad (1)$$

where f_{dn} is the frequency spacing between the grid elements, f_{start} is the starting frequency of the frequency grid. The value of the n-th bit b_n determines the subcarrier of the n-th pair to be used in the output signal. This modulation can be described as

$$s(t) = \sum_{n=1}^{N} sin(2\pi t f_{mesh_{2(n-1)+b_n+1}} + \phi_n), \quad (2)$$

where b_n is the value of the n-th transmitted bit (0 or 1), t is the time, ϕ_n is the random phase of the n-th bit.

In Fig. 1 is presented a spectrum of an exemplary MBFSK signal with $f_{start} = 160$ Hz, $f_{dn} = 160$ Hz, $N = 3$ in the case of transmitting [0, 1, 0] bits. Dotted vertical lines indicate the frequencies of the [0] bits and dashed lines indicate the frequencies of the [1] bits. In addition, the gray area marks the band with a width of $2f_{dn}$ for the second bit. Example spectrum of one transmitted signal package and signal structure along time and frequency was presented by Czapiewska *et al.* (2024a).

Under multipath conditions, after a single symbol has been transmitted, the signal still reverberates through the transmission medium. This time is highly dependent on the basin. Continuous transmission of MBFSK symbols under such conditions will cause ISI (inter-symbol interference), which manifests itself as a superposition of the spectra of adjacent symbols. During the demodulation process, this can cause spurious signal detection at the subcarrier frequency of the bit from the previous symbol instead of the current symbol. To avoid this phenomenon, a guard time T_g between symbols has been implemented.

For the analysis performed in this article, a signal with the following parameters was used: $f_{start} = 65$ kHz, $f_{dn} = 160$ Hz, $N = 250$, $T_g = 100$ ms, and symbol duration $T = 50$ ms. This configuration resulted in a signal with a bandwidth of $2Nf_{dn} = 2 \cdot 250 \cdot 160\ Hz = 80\ kHz$ located between 65 kHz and 145 kHz with a bit rate of $N/(T_g + T) = 250bit/(0.1s + 0.05s) \approx 1667bit/s$.

3. Doppler shift determination methods

The signal described in the previous section is a broadband signal with a center frequency of 105 kHz and a bandwidth of 80 kHz. The Doppler frequency shift phenomenon depends on the operating frequency, speed of the transmitter or receiver, and the speed of sound propagation in the medium used. This phenomenon is described as

$$\Delta f = (\frac{c \pm v_r}{c \mp v_s} - 1)f_0, \quad (3)$$

where Δf is the frequency shift, f_0 is the operating frequency, v_r is the speed of the receiver (positive for approaching, negative for departing), v_s is the speed of the source (positive for departing, negative for approaching) (Halliday *et al.*, 2013). The speed of sound in water c depends on temperature, salinity, and depth. For theoretical considerations, it can be rounded to a value of 1500 m/s (Bjørnø and Buckingham, 2017). With this speed of sound and a transmitter speed of 1 m/s, there is a frequency shift of 43 Hz at the beginning of the transmitted bandwidth $f_0 = 65$ kHz, and a frequency shift of 97 Hz at the end of the bandwidth $f_0 = 145$ kHz. The large difference in the Doppler shifts at the edges of the band forces an analysis based on the frequency-independent Doppler factor μ, expressed as

$$\mu = \frac{c \pm v_r}{c \mp v_s}. \quad (4)$$

To reduce the influence of the Doppler effect on received signals, two methods of estimating the Doppler coefficient have been developed and tested: the correlation method and the double DFT method. The time synchronization is assumed for both of the methods described below.

3.1. Correlation. Performing a normalized cross-correlation between two waveforms returns a function whose maximum determines the degree of similarity between the waveforms. If the analyzed waveforms are identical, the maximum will tend toward unity. If one of the waveforms is distorted, for example, due to multipath or the Doppler effect, the value of the maximum of the correlation will decrease. Since the Doppler effect causes the duration of the received signal and its carrier frequency to be inconsistent with the transmitted signal, the mentioned property of the cross-correlation function can be used to determine the Doppler factor. In the case of MBFSK modulation, where the original frequency grid is known, it is possible to generate a reference spectrum $S_{Ex}(f)$. Such a spectrum is a sequence of subcarriers containing all the elements of the frequency grid $\boldsymbol{f_{mesh}}$. By modifying the reference spectrum by selected Doppler factors μ, it is possible to create a set of reference spectra that take into account the different speeds of reciprocal motion of objects. By correlating the set of reference spectra created in this way with the spectrum of the received signal, it is possible to determine for which value of μ the correlation coefficient will have the highest maximum value. This value of μ should ensure the reduction of the influence of the Doppler effect on the received signal, which should result in the highest quality of reception. The described procedure requires considerable computational effort, mainly due to the need to repeatedly determine the cross-correlation and search for the maximum. This can be greatly simplified by creating appropriate reference frequency grids and summing the values of the amplitude spectrum of the received signal $|S_{MBFSK}|$ at the points of these grids. This allows the determination of a value that can be regarded as equivalent to the correlation coefficient. The maximum value of the sums, for different μ, corresponds to the Doppler shift of the received signal. The algorithm of the method is shown in Algorithm 1. Here f_r is the frequency resolution of the MBFSK (spectrum of the registered signal with L samples, i.e., $f_r = F_s/L$) , which is equivalent to $I_F = I_{f_{start}} + [0, I_{f_{dn}}, 2I_{(f_{dn}}, \ldots, (2N-1)I_{f_{dn}}]$, $I_{f_{start}}$ is the index of the starting frequency of the frequency grid, $I_{f_{dn}}$ is the index spacing between the elements of the frequency grid $\boldsymbol{f_{mesh}}$, μ_{start} is the first expected factor corresponding to the maximum speed of departure, μ_{step} is the resolution of the factor search, and N_μ is the number of searched Doppler factors.

Algorithm 1. Correlation method.

Step 1. Calculate the amplitude spectrum of the received MBFSK symbol.

Step 2. Generate reference frequency grid indices $I_F = \boldsymbol{f_{mesh}}/f_r$.

Step 3. Generate a set of expected Doppler factors $\mu_{chk} = \mu_{start} + [0, \mu_{step}, 2\mu_{step}, \ldots, (N_\mu - 1)\mu_{step}]$.

Step 4. Add up the values of the spectral components of the received signal at the specified indices $C[\mu] = \sum_{f \in I_F} |S_{MBFSK}[f \cdot \mu]|, \mu \in \mu_{chk}$.

Step 5. Find the index of the maximum of the set of sums of the values of the spectral components $i_{max} = \max(C[\mu])$.

Step 6. Read the estimated value of the Doppler factor μ_{est} from the μ_{chk} vector corresponding to the maximum found $\mu_{est} = \mu_{chk}[i_{max}]$.

3.2. Double DFT. The spectrum module of the MBFSK symbol, containing a sequence of zeros or $|S_{MBFSK}(f)|$, can be compared to a comb function with a period, in the frequency domain, of $2f_{dn}$. The Doppler phenomenon changes the frequencies of the received subcarriers by a factor μ, which causes a change in the spacing between them. The change in this spacing can be used to estimate the factor μ, because the spectrum of the original comb function, is also a comb function (Grami, 2016) described by Eqn. (5), in which the spacing between peaks depends on the spacing between peaks of the original comb function $2f_{dn}$. In our case the original comb function is the spectrum of the MBFSK symbol. In this case, we treat the original spectrum analogously to a time course:

$$\mathcal{F}\{\sum_{n=-\infty}^{\infty} \delta(f - 2nf_{dn})\} = \frac{1}{2f_{dn}} \sum_{n=-\infty}^{\infty} \delta(f_f - \frac{n}{2f_{dn}}), \quad (5)$$

where f_f is a variable in the domain after second DFT, $\delta()$ indicates Dirac delta function.

The spectrum of the MBFSK symbol is characterised by a regularity of repeating subcarriers. According to the above, in order to determine this regularity, we perform a second DFT on the spectrum of the MBFSK symbol.

To increase the resolution of the result of the second DFT, the length of the first spectrum can be artificially increased by adding a sequence of zeros. The index of peak occurrence in the result of the second DFT of such signal, in the absence of Doppler effect, can be calculated as

$$k_{m11} = \frac{mMf_r}{2f_{dn}}, \quad (6)$$

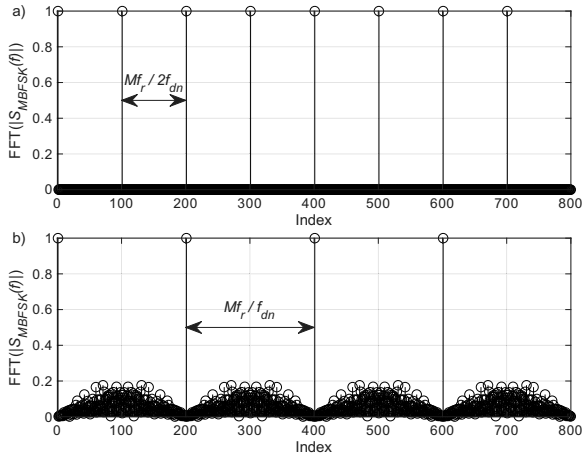

Fig. 2. Double Fourier transform of the MBFSK signal with $M = 800$, $f_r = 20$ Hz, and $f_{dn} = 80$ Hz transmitting: a sequence of ones (a), random data (b).

where m is the peak number and M is the number of elements in the result of the second DFT. A case of a result of the second DFT of the MBFSK symbol containing a sequence of ones is shown in Fig. 2(a).

However, the chance that during transmission, the transmitted data will be a sequence of 0 or 1 is very small. The MBFSK spectrum of the data only resembles a comb function, as there is no regularity in the occurrence of peaks. Nevertheless, in the result of the second DFT there will be dominant peaks with k_m indices, as presented in Fig. 2(b), at intervals of twice that size. The index at which the peak should occur, in the absence of the Doppler effect, can be calculated as

$$k_m = \frac{mMf_r}{f_{dn}}. \tag{7}$$

By comparing the index of the m-th peak, determined for the case without the influence of the Doppler effect (7), with the read index for the maximum of the double spectrum of the signal received for the m-th peak, an estimate of the Doppler factor μ can be determined as

$$\frac{k_m}{k_{mR}} = \frac{\frac{mMf_r}{f_{dn}}}{\frac{mMf_r}{\mu f_{dn}}} = \frac{\mu f_{dn}}{f_{dn}} = \mu, \tag{8}$$

where k_{mR} is the index of the maximum of the double spectrum of the signal received for the m-th peak.

It is important to note that the differences between k_m and k_{mR} are greater greater the value of m. With limited resolution of the result of the second DFT, the accuracy of the estimation can be increased by selecting peaks with as high value of m as possible. However, the number of peaks in the result of the second DFT is limited by the ratio of the spacing between the subcarriers f_{dn}, and the resolution of the first spectrum f_r. The maximum number of peaks useful for estimating the Doppler factor, taking into account the symmetry of the spectrum, can be calculated as

$$m_{Max} = \lfloor \frac{f_{dn}}{2f_r} \rfloor. \tag{9}$$

The resolution of the method μ_{Res} can be calculated using the number of elements M and the peak number m, as

$$\mu_{Res} = \left| 1 - \frac{k_m}{k_m - 1} \right| = \left| 1 - \frac{\frac{Mmf_r}{f_{dn}}}{\frac{Mmf_r}{f_{dn}} - 1} \right| = \left| 1 - \frac{1}{1 - \frac{f_{dn}}{Mmf_r}} \right|, \tag{10}$$

from which equation (11) can be derived, which gives the M required to obtain a given μ_{Res} resolution at the assumed peak number m

$$M = \frac{f_{dn}(\frac{1}{\mu_{Res}} + 1)}{f_r m}. \tag{11}$$

The algorithm of the method is shown in Algorithm 2.

Algorithm 2. Double DFT method.

Step 1. Calculate the amplitude spectrum of the received MBFSK symbol.

Step 2. Trim the first spectrum to the frequency range $f_{start} - 2f_{dn}$ to $f_{start} + (2N + 1)f_{dn}$.

Step 3. Increase the number of components to the M by using a zero padding.

Step 4. Compute the second DFT.

Step 5. Use equation (6) to calculate the index of the peak used for Doppler effect estimation.

Step 6. Find the index of the maximum value in the vicinity of the peak calculated in the previous step.

Step 7. Use equation (8) to calculate the Doppler factor.

4. Measurement setup

The measurements were carried out in the freshwater towing tank at the Faculty of Mechanical Engineering and Shipbuilding at the Gdańsk University of Technology, shown in Fig. 3. This tank is 4 m wide, 40 m long and the water is 3 m deep. Above the pool is a mobile platform with a transmitting transducer submerged to a depth of 1 m. In the towing tank there are difficult sound propagating conditions, because of strong multipath effects. A detailed description of the propagation conditions together with the sequentially recorded forms of the impulse responses is contained in the work of Czapiewska *et al.* (2022). Transmitting transducer was placed in a braced steel mast as shown in Fig. 4. On the other side of the pool, 4 receiving

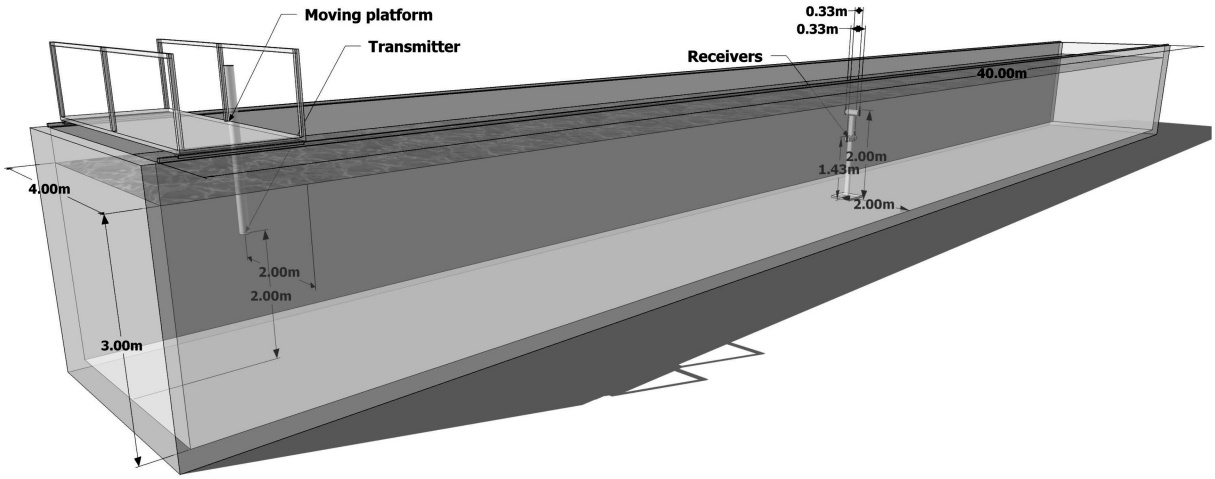

Fig. 3. Schematic of the freshwater towing tank with the measure equipment (Czapiewska *et al*., 2024a).

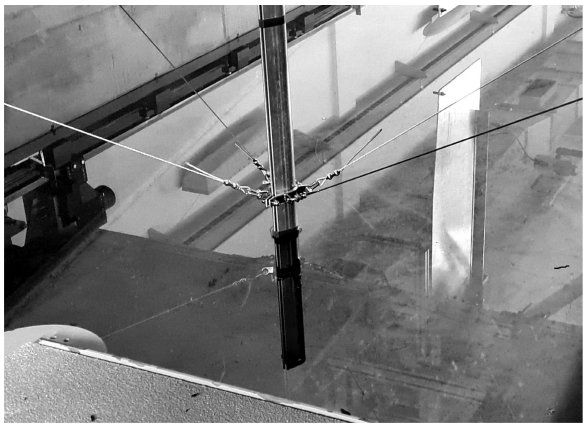

Fig. 4. Mast containing the transmitting transducer (Czapiewska *et al*., 2024a).

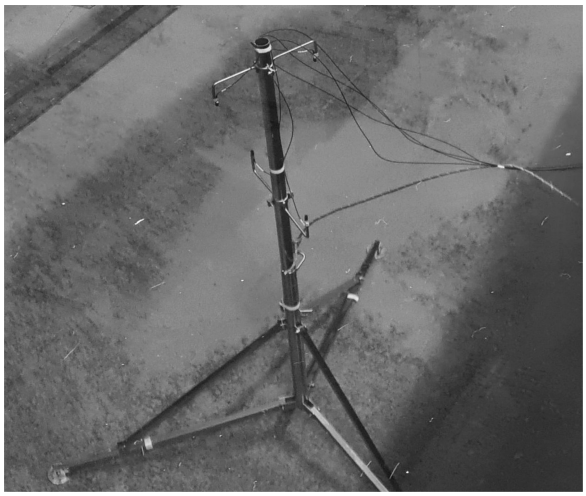

Fig. 5. Support stand with the receiving transducers (Czapiewska *et al*., 2024a).

transducers were placed on a support stand at depths of 1 and 1.57 m, as shown in Fig. 5. The distance between the receiving transducers placed at the same depth was 0.33 m. During the course of the measurements, the Reson TC4013 transducers were driven by the ETEC PA1001 power amplifier on the transmitting side, and the ETEC A1105A power amplifier on the receiving side. The signal was generated and collected using the National Instruments USB-6366 device.

Measurements were carried out at speeds of 1.5, 1, and 0.5 m/s with an accuracy of 0.01 m/s for f_{dn} equal to 160 Hz. For each speed measurements on 6 runs from the transmitter to the receiver were performed. By treating the signal received simultaneously on the 4 receiving transducers as independent transmissions, a set of 24 measurements was obtained for each speed tested.

In the tank used, the speed of sound was measured with the Valeport SWIFT CTD plus probe and $c = 1476$ m/s was obtained. The theoretical value of the Doppler factor μ, obtained using Eqn. (4) for the speeds at which measurements were made, are 1.00102 for 1.5 m/s, 1.00068 for 1 m/s, and 1.00034 for 0.5 m/s, although, according to our previous studies, the most optimal value of the Doppler factor, in terms of the lowest bit error rate, lower than indicated by the aforementioned value calculated based on information about the speed of the transmitter relative to the receiver (Czapiewska *et al*., 2024a).

5. Results

This section presents the BER (Bit Error Rate) results obtained from the tests after applying a frequency shift correction based on the estimated Doppler factor μ. Only the portion of each run where the distance between the transmitter and receiver was between 3 and 10.6 meters was included in the analysis. In this portion of each run, 35 symbols were transmitted for a speed of 1.5 m/s, 52 symbols were transmitted for a speed of 1 m/s, and 103 symbols were transmitted for a speed of 0.5 m/s. Since data was collected from 24 measurements and each symbol consisted of 250 bits, the resulting BER was determined to 210 kbits for 1.5 m/s speed, 320 kbits for 1 m/s speed, and 618 kbits for 0.5 m/s speed.

The parameters of each of the methods tested were chosen to provide an estimate of Doppler factor μ with an accuracy of 0.00001 in the range corresponding to speeds from -1.6 to 1.6 m/s with a measured sound velocity of 1476 m/s. For the correlation method, this results in a range of expected μ_{chk} values from 0.99892 to 1.00108. For the double DFT method, 3 pairs of test parameters were assumed: $M_1 = 800008$, $m_1 = 1$; $M_2 = 400004$, $m_2 = 2$; $M_3 = 266669$, $m_3 = 3$.

In the correlation method, the effect of the number of bits used N_B and the band of the subcarriers B used on the result of the Doppler factor μ estimation was studied. The number of subcarriers used was modified by omitting the use of every nth bit from the set in the index calculation process, while the bandwidth was modified by selecting only the 9 leading, middle or trailing bits, respectively low band 65–67.9 [kHz], middle band 103.4–106.3 [kHz] and high band 142.1–145 [kHz].

In the double DFT method, the effect of the number of peaks m used, while keeping the resolution of the result of the second DFT constant, on the result of the Doppler factor μ estimation was investigated. The number of elements of the result of the second DFT M was increased by adding zeros to the spectrum of the received signal.

Table 1 shows the BER values for all tested configurations of the correlation method. It can be seen that, considering the number of bits used, the best results for speeds of 1.5 and 1 m/s were obtained using all 250 bits. As the number of bits decreases, the BER increases sharply, which is due to the large estimation error. Fig. 6 shows the Doppler factor μ as a function of the distance between the transmitter and receiver for 250 and 50 N_B used in the correlation method estimation at a speed of 1.5 m/s on a single hydrophone. Estimates with both configurations have similar values, but there are individual errors when using 50 bits. Reducing the number of bits further increases the number of large errors in the μ estimation, resulting in a higher BER.

The large deviations of the μ values from the expected ones, shown in Fig. 6, are due to the fact that the

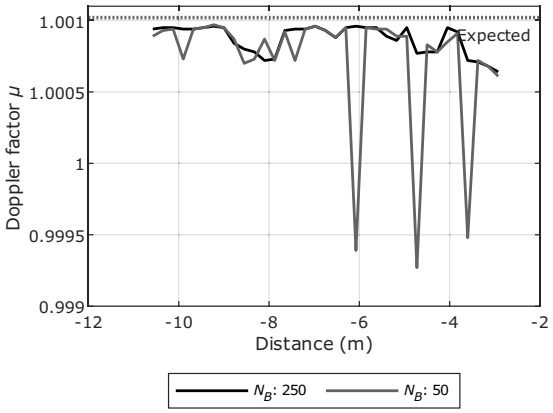

Fig. 6. Doppler factor μ as a function of the distance between the transmitter and receiver for 250 and 50 N_B used in the correlation method estimation at 1.5 m/s speed on a single transducer. The horizontal dotted line shows the Doppler factor value calculated from Eqn. (4).

smaller the number of bits used to estimate the Doppler factor, the fading of at least one of the bits causes larger estimation errors. In addition, the assumed frequency grid has a constant frequency spacing, so the Doppler frequency shift can occur, which can cause a problem in recognizing the components predicted for 0 and 1. The probability of such an event is higher in the range of higher frequencies than in the range of lower frequencies, because at the lower frequencies the Doppler shift is smaller compared to f_{dn}.

Assuming an initial estimate, at least of the direction of motion, it is possible to reduce the range of Doppler factors sought. A re-estimation of the Doppler factor was performed by selecting a set of predicted μ_{chk} values that did not account for the object moving away. A significantly lower bit error rate was obtained, as shown in Table 2. BER values that are identical to those shown in Table 1 are underlined. Using all the bits or only the lower part of the bandwidth does not require an initial estimation. After reducing the search range, the estimation did not exceed the value of BER 10^{-3}.

The results as a function of the bandwidth of the subcarriers used do not show any specific relationship, the BER values obtained are comparable. However, it is worthwhile to analyze the BER as a function of the frequency at which the bits are transmitted, as shown in Fig. 7. It can be seen that using the lower band to estimate μ, the lowest number of errors was obtained in the lower band, but at the same time the highest in the upper band. Similarly, μ determined using the upper band gives the lowest BER values in the upper band and higher values in the lower band. This may indicate the need for separate determination of the Doppler factor in the subbands. Table 3 shows the BER values for all tested configurations of the double DFT method. It can be seen

Table 1. BER values for all tested configurations of the correlation method.

Number of bits N_B used	BER at v 1.5 m/s	BER at v 1 m/s	BER at v 0.5 m/s
250	$8.05e-04$	$4.39e-04$	$2.10e-05$
50	$2.52e-02$	$2.46e-03$	$2.10e-05$
9	$8.92e-02$	$5.34e-02$	$3.65e-02$
5	$1.07e-01$	$9.62e-02$	$8.18e-02$
9 (low band)	$7.43e-04$	$5.10e-04$	$1.62e-05$
9 (middle band)	$1.90e-01$	$2.26e-01$	$8.39e-02$
9 (high band)	$2.42e-01$	$2.06e-01$	$2.39e-01$

Table 2. BER values for all tested configurations of the correlation method assuming initial estimation and reducing the search range μ to $1-1.00108$.

Number of bits N_B used	BER at v 1.5 m/s	BER at v 1 m/s	BER at v 0.5 m/s
250	$8.05e-04$	$4.39e-04$	$2.10e-05$
50	$8.48e-04$	$4.20e-04$	$2.10e-05$
9	$7.48e-04$	$3.43e-04$	$1.78e-05$
5	$6.05e-04$	$3.65e-04$	$1.78e-05$
9 (low band)	$7.43e-04$	$5.10e-04$	$1.62e-05$
9 (middle band)	$6.67e-04$	$3.97e-04$	$1.94e-05$
9 (high band)	$7.00e-04$	$3.37e-04$	$1.36e-03$

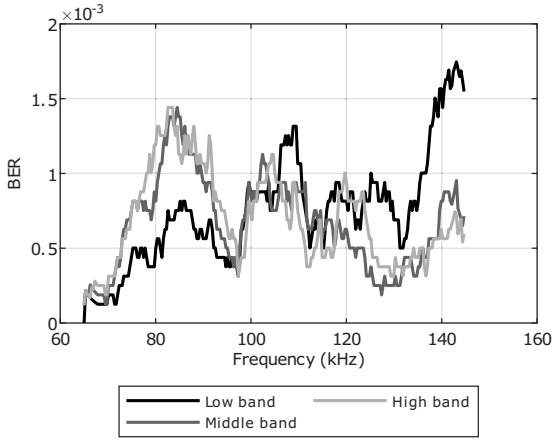

Fig. 7. BER as a function of the bits frequency for different bands used for the correlation method estimation μ at 1.5 m/s speed.

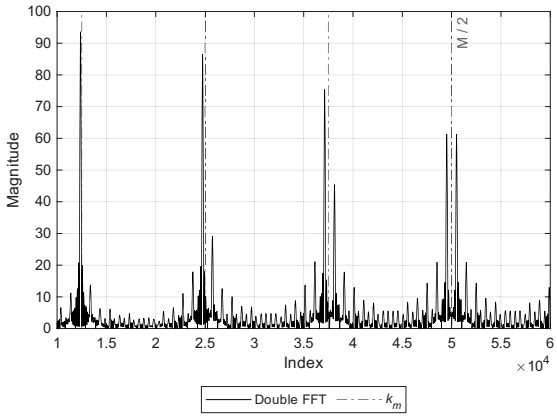

Fig. 8. Simulation of the double DFT spectrum affected by the Doppler effect.

that using the peak with the smaller index results in lower BER than the following peaks. This is caused by the interaction of the peaks from the overlapped spectrum components. The best results are obtained for a value of m equal to 1, where the influence of the overlapped spectrum is the least. The situation of such spectrum interaction is shown in Fig. 8, which shows the simulation of the Double DFT spectrum affected by the Doppler effect. The vertical lines indicate the index positions of the peaks k_m without the influence of the Doppler effect. The peaks corresponding to the approaching speed are to the left of the dotted lines, but peaks occurring to the right can also be seen. In the case where the quotient f_{dn}/f_r is not a whole number, the peaks of the fundamental and the overlapped spectrum do not appear on the same spectral components. This results in the observation of two peaks near the expected k_m component, which can lead to errors in the estimation of μ. This interaction is stronger the higher the value of m.

A comparison of the bit error rate values obtained by the two methods, with parameters that had the lowest BER, shows that they have very similar results. However, it should be noted that the reduction of bits in the correlation method is associated with the risk of a large estimation error. The computational complexity of the

Table 3. BER values for all tested configurations of the double DFT method.

Parameters	BER at v 1.5 m/s	BER at v 1 m/s	BER at v 0.5 m/s
$M = 800008, m = 1$	$5.95e-04$	$6.51e-04$	$1.94e-05$
$M = 400004, m = 2$	$9.46E-03$	$1.42E-03$	$1.94E-05$
$M = 266669, m = 3$	$9.60E-02$	$2.89E-02$	$1.78E-05$

Table 4. Measured average methods times.

Method	Time [ms]
Correlation, $N_B = 5$	0.079
Correlation, $N_B = 9$	0.081
Correlation, $N_B = 50$	0.150
Correlation, $N_B = 250$	0.509
Double DFT, $M = 800008, m = 1$	9.109
Double DFT, $M = 400004, m = 2$	7.565
Double DFT, $M = 266667, m = 3$	6.379

correlation method is much lower than that of the double DFT method, as shown in Table 4. The methods' times were determined as the average time of 1068 function calls and was performed using Matlab environment on Intel i5-13500 processor with RAM bandwidth of 3600 MT/s.

6. Conclusions

This article compares two methods for determining the Doppler frequency shift applicable to the MBFSK modulation. The advantage of both correlation and double DFT methods is that they do not require the use of additional signals at the expense of the bandwidth allocated for this transmission. There is no need for additional signals, such as pilots, to determine the frequency shift caused by motion. The reception quality expressed as BER obtained using pilots (Czapiewska *et al*., 2024b), is comparable to the methods described in this paper, but does not require additional bandwidth that can be used for data transmission. Both methods use only the useful signal, i.e., the transmitted information. The frequency shifts determined by these methods correspond to the conditions at the time of reception individually for each symbol. A comparison of these methods shows that they provide comparable reception quality. However, the double DFT method requires significantly more computation. On the other hand, the disadvantage of the correlation method is the possibility of a large error in the estimation of the Doppler coefficient, which leads to a wrongly received symbol. This is due to selective fading. This error can be avoided by narrowing the range of Doppler coefficient values in the initial estimation. The double DFT method does not have this disadvantage. However, due to the high computational complexity, it cannot always be used in autonomous systems. It should be expected that there will be different Doppler shifts in different subbands. In the course of the study, the influence of Doppler induced inter-bit-interference phenomena was noted. The problem of Doppler scattering will be the subject of further study. Accurate estimation of the frequency shift is essential to ensure high bit-rate (small spacing between subcarriers) and high quality (low BER) communications.

Acknowledgment

This work was supported by the National Centre for Research and Development under the project DOB-SZAFIR/01/B/017/04/2021.

We would like to thank the Faculty of Mechanical Engineering and Ship Technology of the Gdańsk University of Technology for the opportunity to conduct research in the towing tank.

References

Baldone, C., Galioto, G.E., Croce, D., Tinnirello, I. and Petrioli, C. (2020). Doppler estimation and correction for JANUS underwater communications, *GLOBECOM 2020 IEEE Global Communications Conference, Taipei, Taiwan*, pp. 1–6.

Bjørnø, L. and Buckingham, M. (2017). General characteristics of the underwater environment, *in* T.H. Neighbors and D. Bradley (Eds), *Applied Underwater Acoustics*, Elsevier, Amsterdam, pp. 1–84.

Czapiewska, A., Luksza, A., Studanski, R. and Zak, A. (2022). Analysis of impulse responses measured in motion in a towing tank, *Electronics* **11**(22), Article no. 3819.

Czapiewska, A., Łuksza, A., Studański, R., Wojewódka, L. and Żak, A. (2024a). Comparison of Doppler effect estimation methods for MFSK transmission in multipath hydroacoustic channel, *IEEE Access* **12**: 49976–49986.

Czapiewska, A., Łuksza, A., Studański, R., Wojewódka, L. and Żak, A. (2024b). Evaluating the effectiveness of Doppler frequency shift determination using pilots in broadband transmission, *International Journal of Electronics and Telecommunications* **70**(4): 797–803.

Deguchi, M., Kida, Y. and Shimura, T. (2022). Suppression of effects of Doppler shifts of multipath signals in underwater acoustic communication, *Acoustical Science and Technology* **43**(1): 10–21.

Diamant, R., Feuer, A. and Lampe, L. (2012). Choosing the right signal: Doppler shift estimation for underwater acoustic signals, *Proceedings of the 7th International Conference*

on Underwater Networks & Systems, New York, USA, pp. 1–8.

Eynard, G. and Laot, C. (2008). Blind Doppler compensation scheme for single carrier digital underwater communications, *OCEANS 2008, Quebec City, Canada*, pp. 1–5.

Grami, A. (2016). Signals, systems, and spectral analysis, *in* A. Grami (Ed.), *Introduction to Digital Communications*, Academic Press, Boston, pp. 41–150.

Halliday, D., Resnick, R. and Walker, J. (2013). *Fundamentals of Physics, Extended*, Wiley, Hoboken.

Jin, Q., Wong, K.M. and Luo, Z.-Q. (1995). The estimation of time delay and Doppler stretch of wideband signals, *IEEE Transactions on Signal Processing* **43**(4): 904–916.

Johnson, M., Freitag, L. and Stojanovic, M. (1997). Improved Doppler tracking and correction for underwater acoustic communications, *1997 IEEE International Conference on Acoustics, Speech, and Signal Processing, Munich, Germany*, pp. 575–578.

Li, B., Zheng, S. and Tong, F. (2019). Bit-error rate based Doppler estimation for shallow water acoustic OFDM communication, *Ocean Engineering* **182**: 203–210.

Li, B., Zhou, S., Stojanovic, M., Freitag, L. and Willett, P. (2008). Multicarrier communication over underwater acoustic channels with nonuniform Doppler shifts, *IEEE Journal of Oceanic Engineering* **33**(2): 198–209.

Liu, Y., Zhao, Y., Gerstoft, P., Zhou, F., Qiao, G. and Yin, J. (2023). Deep transfer learning-based variable Doppler underwater acoustic communications, *The Journal of the Acoustical Society of America* **154**(1): 232–244.

Ma, L., Jia, H., Liu, S. and Khan, I.U. (2020). Low-complexity Doppler compensation algorithm for underwater acoustic OFDM systems with nonuniform Doppler shifts, *IEEE Communications Letters* **24**(9): 2051–2054.

Mason, S.F., Berger, C.R., Zhou, S. and Willett, P. (2008). Detection, synchronization, and Doppler scale estimation with multicarrier waveforms in underwater acoustic communication, *IEEE Journal on Selected Areas in Communications* **26**(9): 1638–1649.

Misiurewicz, J., Bruliński, K., Klembowski, W. and Kulpa, K. (2021). Multipath propagation of acoustic signal in a swimming pool, *2021 Signal Processing Symposium (SPSympo), Łódź, Poland*, pp. 197–201.

Mizeraczyk, J., Studanski, R., Zak, A. and Czapiewska, A. (2021). A method for underwater wireless data transmission in a hydroacoustic channel under NLOS conditions, *Sensors* **21**(23), Article no. 7825.

Nguyen, V.D., Thi, H. L.N., Nguyen, Q.K. and Nguyen, T.H. (2022). Low complexity non-uniform FFT for Doppler compensation in OFDM-based underwater acoustic communication systems, *IEEE Access* **10**: 82788–82798.

Ostrowski, Z., Salamon, R., Kochańska, I. and Marszal, J. (2020). Underwater navigation system based on Doppler shift—Measurements and error estimations, *Polish Maritime Research* **27**(1): 180–187.

Perrine, K.A., Nieman, K.F., Henderson, T.L., Lent, K.H., Brudner, T.J. and Evans, B.L. (2010). Doppler estimation and correction for shallow underwater acoustic communications, *2010 Conference Record of the 44th Asilomar Conference on Signals, Systems and Computers, Pacific Grove, USA*, pp. 746–750.

Sharif, B., Neasham, J., Hinton, O. and Adams, A. (1999). Doppler compensation for underwater acoustic communications, *MTS/IEEE Oceans'99 Conference and Exhibition: Riding the Crest into the 21st Century, Seattle, USA*, pp. 216–221.

Sharif, B., Neasham, J., Hinton, O. and Adams, A. (2000). A computationally efficient Doppler compensation system for underwater acoustic communications, *IEEE Journal of Oceanic Engineering* **25**(1): 52–61.

Sun, D., Hong, X. and Cui, H. (2022). A Kalman-based Doppler tracking algorithm for underwater acoustic spread spectrum communications, *Applied Acoustics* **185**: 108374.

Sun, D., Hong, X., Cui, H. and Liu, L. (2020). A symbol-based passband Doppler tracking and compensation algorithm for underwater acoustic DSSS communications, *Journal of Communications and Information Networks* **5**(2): 168–176.

Sun, D., Wu, J., Hong, X., Liu, C., Cui, H. and Si, B. (2023). Iterative double-differential direct-sequence spread spectrum reception in underwater acoustic channel with time-varying Doppler shifts, *Journal of the Acoustical Society of America* **153**(2): 1027–1041.

Talarczyk, T. (2023). A dynamic submerging motion model of the hybrid-propelled unmanned underwater vehicle: Simulation and experimental verification, *International Journal of Applied Mathematics and Computer Science* **33**(2): 207–218, DOI: 10.34768/amcs-2023-0016.

Wada, T., Suzuki, T., Yamada, H. and Nakagawa, S. (2016). An underwater acoustic 64QAM OFDM communication system with robust Doppler compensation, *OCEANS 2016, Monterey, USA*, pp. 1–4.

Wei, R., Ma, X., Zhao, S. and Yan, S. (2020). Doppler estimation based on dual-HFM signal and speed spectrum scanning, *IEEE Signal Processing Letters* **27**: 1740–1744.

Zhao, S., Yan, S. and Xu, L. (2019). Doppler estimation based on HFM signal for underwater acoustic time-varying multipath channel, *2019 IEEE International Conference on Signal Processing, Communications and Computing (ICSPCC), Dalian, China*, pp. 1–6.

Agnieszka Czapiewska works in the Department of Radiocommunication Systems and Networks at the Faculty of Electronics, Telecommunications and Informatics of the Gdańsk University of Technology as an assistant professor. Her PhD thesis concerns the indoor radiolocalization research area. Her scientific interests cover topics in radiocommunications systems and networks, radiolocalization, signal processing, and recently of physical layer of underwater acoustic digital communication in shallow waters.

Andrzej Łuksza was born in Gdańsk, Poland, in 1959. He received his BSc-MSc in electronics in 1984 from the Gdańsk University of Technology and his PhD in 1998 from the same university. From 1984 to 1998 he was an assistant lecturer with the Department of Marine Telecommunications, Gdynia Maritime University, Poland. Since 1998 he has been an assistant professor there. His research includes digital signal processing, underwater communication and neural networks.

Jan H. Schmidt is a graduate of the Faculty of Electronics, Telecommunications and Computer Science at the Gdańsk University of Technology. He holds a master's degree in automation and robotics, specializing in the automation of moving objects. In 2018, he obtained a PhD in the field of telecommunications. He currently works as an assistant professor at the Department of Signals and Systems of the Gdańsk University of Technology. His scientific interests include hydroacoustics, in particular underwater communication, active and passive sonars.

Ryszard Studański obtained his PhD at the Faculty of Electronics, Telecommunications and Computer Science of the Gdańsk University of Technology in 2003. He has been working as an assistant professor at the Naval Academy since 2003 and at the Maritime University of Gdynia since 2014. He is interested in the problems of analyzing signals recorded in a wide band.

Łukasz Wojewódka was born in Wejherowo, Poland, in 1998. He received his BSc and MSc degrees in electronics and telecommunications from Gdynia Maritime University, Poland, in 2022 and 2023, respectively. He is currently pursuing a PhD degree in automation, electronics, electrical engineering and space technologies at that university. Also, since 2023, he has been an assistant lecturer with the Department of Marine Telecommunications there. His research interests include underwater communication.

Andrzej Żak was born in Warsaw, Poland, in 1977. He received his MSEng degree in information technology from the Military University of Technology in Warsaw in 2001, his PhD degree in mechanical engineering from the Polish Naval Academy in 2006, and in 2015, the AGH University of Science and Technology awarded him a DSc degree in technical sciences in the field of automation and robotics with the specialization in lecture autonomous underwater vehicles. Since 2003 he has been working at the Polish Naval Academy, first in the Hydroacoustics Department and now in the Information Technology Department as an associate professor and the department head. He has participated in more than 20 research and development projects and has published more than 100 papers and articles. His research interests include firstly passive observation of the physical fields of ships, especially hydroacoustics. In recent years he has concentrated on underwater wireless communications using elastic waves in hard propagation conditions.

Received: 13 September 2024
Revised: 24 January 2025
Re-revised: 7 March 2025
Accepted: 10 March 2025